Materials Science and Engineering C 32 (2012) 478–486

Contents lists available at SciVerse ScienceDirect

Materials Science and Engineering C

journal homepage: www.elsevier.com/locate/msec

Biological hydroxyapatite obtained from fish bones

M. Boutinguiza [a], J. Pou [a,*], R. Comesaña [a], F. Lusquiños [a], A. de Carlos [b], B. León [a]

[a] Applied Physics Dpt., Universidade de Vigo, E.T.S.I.I., Lagoas-Marcosende, E-36310, Vigo, Spain
[b] Biochemistry, Genetics and Immunology Dpt., Universidade de Vigo, Facultad de Biología, Lagoas-Marcosende, E-36310, Vigo, Spain

ARTICLE INFO

Article history:
Received 24 October 2010
Received in revised form 19 September 2011
Accepted 28 November 2011
Available online 3 December 2011

Keywords:
Hydroxyapatite
Biological apatite
Calcium phosphate
Fish bones

ABSTRACT

In this study biological HA has been obtained from fish bones, which are available as waste from fishing activities. Fish bone can be used as a cheap source of biological HA contributing at the same time to give added value to fishing by-products as well as reducing the undesirable environmental impact. For this purpose, fish bones of sword fish and tuna have been cleaned and subjected to heat treatment. Material obtained at 600 °C is a B type hydroxyapatite. At 950 °C a biphasic material was found: biological hydroxyapatite/beta-TCP in a 87/13 ratio. The in vitro cytotoxicity test assessed that all materials are non-cytotoxic.
These materials present a promising future because the raw material are wastes, while using a biological substituted apatite containing Mg and Sr as bone substitutes, instead of synthetic apatite without them, would be much beneficial for bone defect healing.

© 2011 Elsevier B.V. All rights reserved.

1. Introduction

Globally more than 91 million tons of fish and shellfish are caught each year. The Food and Agricultural Organisation (FAO) estimates that barely about 50–60% of this catch is been used for human consumption, while the rest is considered discard [1]. Huge amounts of by-products or rest of the raw materials are wasted, generating an undesirable environmental impact. Despite the increasing efforts to obtain new goods from the by-products, the major part is still used for animal meal production. To contribute to reduce the overexploitation as well as the adverse environmental effects it would be advisable to aim at the obtaining of products with high added value produced from the rest-raw material. Some fish species are commercialised after extracting the bones such as the frozen-at-sea fillets, and the material considered discard is partially composed by bones. These bones could be used as a cheap source of calcium phosphate.

Hydroxyapatite (HA) and related calcium phosphate ceramic materials have been widely used as implant materials due to their close similarity in composition with natural bone. From a chemical and structural point of view, HA with the stoichiometric formula $Ca_{10}(PO_4)_6(OH_2)$ and a Ca/P molar ratio = 1.67, is the material most similar to the inorganic part of bones and teeth. Both dense and porous HA have been vigorously investigated as implant materials for orthopaedic and dental applications, showing excellent bioactivity, osteoconductivity, and osteoinductivity [2–4]. However there are differences when comparing synthetic and natural hydroxyapatite, the latter has better metabolic activity and more dynamic response to the environment than the synthetic one [4,5]. Solubility and bioactivity of HA are controlled by their crystallographic structure. In contrast to typical synthetic HA, the biological one has disordered nanostructures and nonstoichiometric composition together with less hydroxyl content, where its amount in cortical human bone is about 20% of that in stoichiometric HA [6]. As it is known, materials at nanoscale have different chemical and physical properties which determine its behaviour [7]. Hence, it is logic to expect that biological HA leads to better results as implant or coating material when its nanoscale properties are preserved.

During the last decades much effort has been paid to obtain synthetic hydroxyapatite. Therefore a variety of methods is available at present for this purpose, such as: solid state reaction [8], co-precipitation [9], sol–gel [10], or hydrothermal processing [11]. Nevertheless these methods might be complicated, time consuming and expensive. Biological HA obtained from animal bones presents the advantage to preserve some properties of the precursor material such as chemical composition and structure [12]. Fish bones could be used as a cheap source of natural calcium phosphate. In previous works we obtained calcium phosphate micro and nanoparticles from fish bones [13,14], but the production method was expensive and complex. Other authors used bones from cephalopoda such as cuttlefish (*Sepia officinalis*) to obtain calcium phosphate from calcium carbonate via a hydrothermal transformation [15]. In this paper a simple and cheap method is presented, based on heat treatment to produce great amounts of HA from fish bones. The composition and structure of the obtained powders were characterised. Furthermore, its cytotoxicity has been tested as a first step to assess its use as a bioactive material.

* Corresponding author at: Universidad de Vigo, Departamento de Física Aplicada., E.T.S. Ingenieros Industriales, Lagoas-Marcosende, Spain. Tel.: +34 986 812 216; fax: +34 986 812 201.
E-mail address: jpou@uvigo.es (J. Pou).

0928-4931/$ – see front matter © 2011 Elsevier B.V. All rights reserved.
doi:10.1016/j.msec.2011.11.021

2. Materials and methods

2.1. Fish bones

Fish bones were obtained from different specimens of sword fish (*Xiphias gladius*) and tuna (*Thunnus thynnus*) captured in North Atlantic fishing-grounds. Bones were immediately frozen after being removed from the fish at the factory ships, assuring that the cold chain was not broken at any time. As received frozen bones were boiled in water for 1 h and washed by the use of a strong water jet to remove the organic substances and the adherent fish meat. Thereafter, bones were dried at room temperature in air for 24 h. The dried fish bones were then calcined in a furnace at both 600 and 950 °C at a heating rate of 10 °C/min in air. Once the calcination temperature had been reached, the bones were maintained isothermally for 12 h, and then cooled at 20 °C/min. The calcined samples were milled for 1 min by the use of milling balls.

2.2. Characterization of the powder

The morphology of powders obtained under the mentioned conditions was studied by a field effect scanning electron microscope (JEOL-JSM-6700F) equipped with an EDAX PV 9760 detector for energy dispersive microanalysis (EDX) to analyse local chemical composition.

The detailed morphology and microstructure were examined by a JEOL-JEM 210 FEG transmission electron microscope (TEM) equipped with a slow digital camera scan, using an accelerating voltage of 200 kV. High resolution transmission electron microscopy (HRTEM) images were obtained in thin crystals.

The crystalline structure and the phase composition of the resulting powder were determined using a Siemens D-5000 X-ray diffractometer. Data were collected over the 2θ range 5° to 40°. Identification of phases was achieved by comparing the diffraction patterns of HA with ICDD (JCPDS) standards.

In order to obtain an estimation of the β-TCP content in our powder samples, bi-component mixtures of HA and β-TCP (Plasma-Biotal, UK) with different weight proportions were analysed by XRD according to the method established by standard ISO-13779:3. Integrated intensity ratios of peak 211 of HA and peak 0210 of β-TCP were used for plotting the calibration curve weight/peak integrated intensity ratio [16].

The functional groups obtained at different temperatures were identified by Fourier-transform infrared spectroscopy (FTIR) using a Thermo Nicolet 6700 spectrometer. Spectra were acquired between 400 and 4000 cm^{-1}. The typical acquisition conditions were 4 cm^{-1} of resolution, averaging of 32 scans, an apodization Happ–Genzel, a Mertz phase correction, and zero filling 2.

A Horiba Jobin Yvon LAbRam-HR800 spectrometer provided with an Ar laser excitation source (488 nm) coupled to a microscope was used to obtain Raman spectra from the studied materials. Raman reflection spectra were acquired between 350 and 1800 cm^{-1} with 1 cm^{-1} of resolution. Acquisition settings were 40 s/scan, 15 averaging scans per measured range and 2 μm of spot size.

In order to evaluate Ca/P ratio, as well as the composition and the presence of heavy metals, inductively coupled plasma-optical emission spectrometry (ICP-OES) analysis was performed using a Perkin Elmer Optima 4300 DV spectrometer. Each assay was repeated three times and the results are presented as mean values.

2.3. Cell culture

Mouse calvaria MC3T3-E1 cells from passage 6 were obtained from the European Collection of Cell Cultures (Salisbury, UK). The cells were cultured in alpha minimum essential medium (α-MEM) with nucleotides and glutamine (Lonza) supplemented with 10% of foetal bovine serum (Lonza) without antibiotics, and maintained at 37 °C in a humidified atmosphere with 5% of CO_2.

2.4. Test for in-vitro cytotoxicity of the materials

Samples of obtained powders from fish bones at both temperatures and from commercial hydroxyapatite (Sigma-Aldrich, HA 289396) have been used to assess their cytotoxicity as well as to compare our powders with commercial synthetic HA. Extracts of the test materials were prepared by placing them in powder form on a rotating mixer for 24 h in alpha MEM at 37 °C, following the European Standard EN ISO 10993-12. The mass to volume extraction ratio was 0.1 g to 10 mL. Materials and media were filtered and the extracts diluted with alpha methylthiazol tetrazolium (MTT) to give 100, 50, 20, 10 and 5% of the original concentration. The extracts were used to culture cells at a concentration of 2×10^5 cells mL^{-1}, for 24 h in 96-well tissue culture plates. After the incubation period the MTT [3-(4,5-dimethyltyazolyl-2)-2,5-diphenyl tetrazolium bromide] labelling reagent (Roche) was added to the cells. The mitochondrial enzyme succinate dehydrogenase, present only in viable cells, converts the MTT to a blue coloured formazan crystal. The amount of blue colour is proportional to the number of viable cells. Phenol at a concentration of 6.4 g L^{-1} was used as a positive toxic control. Pure alpha MEM was used as the negative control.

3. Results

FSEM and TEM analysis indicated that the obtained powders are composed of rod-like shape particles with submicron average size. There was no significant difference in the morphological appearance among the samples from the different species and temperatures. The representative morphology of particles is shown in Fig. 1. The HRTEM image of particles shown in Fig. 2 clearly indicates their crystalline character, with a regular spacing of the observed lattice planes of about 0.80 nm. The corresponding Fast Fourier Transform (FFT) indicates the presence of aperiodic spots revealing that the crystal is not monocrystalline. The FFT pattern (Fig. 2b) shows the reflections (0–10) and (−211) along the [102] zone axis corresponding to the interplanar distances of 0.80 and 0.38 nm, in agreement with those of HA (0.82 and 0.39 nm interplanar distances respectively).

Results of elemental composition together with the Ca/P molar ratio of the powders obtained at both temperatures are listed in Table 1. The main components of the powders obtained from both species (Xiph for sword fish and Thun for tuna) are calcium and phosphorus, showing similar concentration of both elements in the different species and an average Ca/P molar ratio around 1.87 ± 0.02, higher than the stoichiometric ratio. Other elements such as sodium, magnesium, potassium and strontium were detected in a much smaller amount, while the concentration of heavy metals in the obtained powders from fish bones was around 5 orders of magnitude lower (Pb: 0.7 mg/kg, Cd: 0.9 mg/kg, Hg<0.1 mg/kg).

The FTIR spectra from all samples calcined at 600 and 950 °C are presented in Figs. 3 and 4 exhibiting narrow bands which suggest a high degree of crystallisation. The spectra show the characteristic bands for PO^{3-}_4 group consisting of three main regions. The first one is represented by the peaks 1093, 1047 cm^{-1} corresponding to v_3 stretching mode and 962 cm^{-1} associated to v_1 stretching mode. The second region of phosphate ions is represented by the v_4 band with well defined peaks at 634, 603 and 571 cm^{-1} corresponding to bending mode. The third region is observed at 474 cm^{-1} exhibiting weak bands corresponding to v_2 bending mode. Hydroxyl stretching mode is observed on all sample spectra at 3573 cm^{-1} represented by a very low intensity peak. Concerning carbonate ions, there are usually three vibrational bands which can be observed in the infrared spectra of bone and carbonate hydroxylapatite, but v_4 bands exhibit very low intensity and are rarely observed [17,18]. In samples calcined at 600 °C carbonate ions are detected at two different sites: a) peak at 875 cm^{-1} and b) peaks from 1639 to 1384 cm^{-1} cm. The

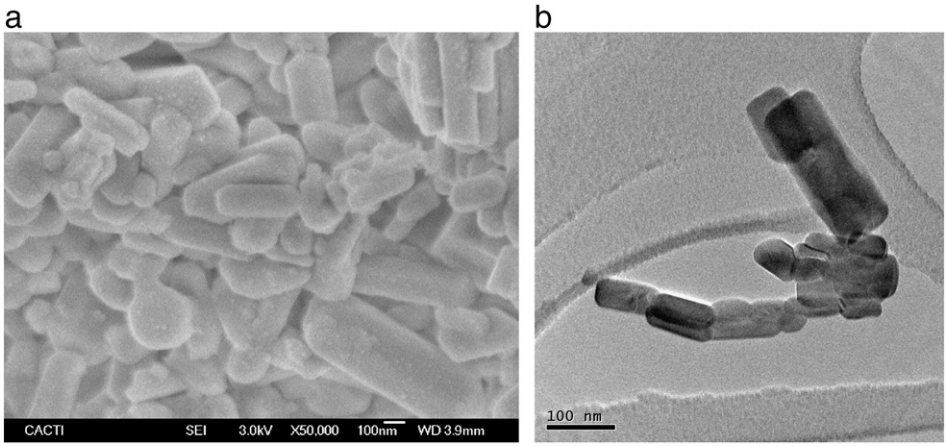

Fig. 1. a) FSEM and b) TEM micrographs showing the appearance of the obtained powders from fish bones at 600 °C.

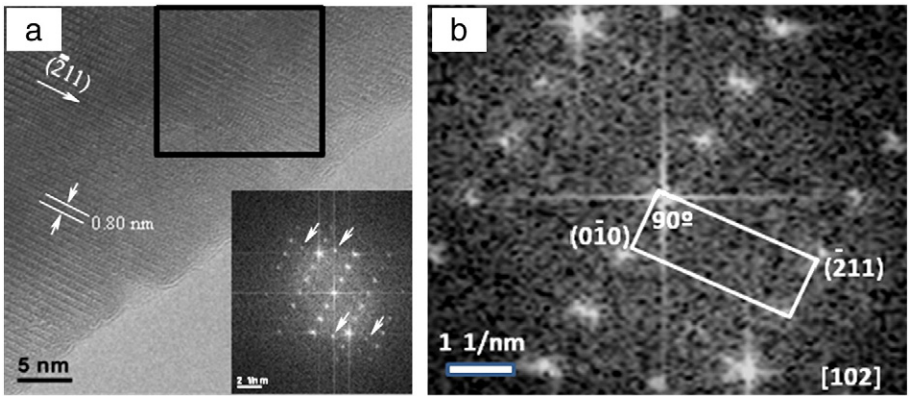

Fig. 2. a) HRTEM image of the side of single particle with the FFT of the framed region showing the presence of aperiodic spots (white arrows). b) The corresponding FFT; notice the presence of the reflections (0–10) and (−211) along the [102] consistent with HA.

presence of organic material (C-H) is detected as low intensity peaks at 2925 and 2852 cm^{-1}.

The Raman spectra obtained from the samples calcined at 600 and 950 °C are dominated by a very strong peak at 962 cm^{-1} related to the PO^{3-}_4 v_1 stretching mode (see Figs. 5 and 6). Medium intensity peaks corresponding to PO^{3-}_4 v_2 bending modes are present at 430 and 447 cm^{-1}; while the v_4 bending modes are found at 579, 591, 607 cm^{-1} and with lower intensity at 615 cm^{-1}. In the band between 1000 and 1100 cm^{-1}, the medium intensity peaks at 1029, 1047, 1076 cm^{-1} are attributed to PO^{3-}_4 v_3 antisymmetric stretching mode, in addition to the contribution at 1073 cm^{-1} of the CO^{-3}_2 $v1$ antisymmetric stretching mode [19,20]. In the case of the Xiph calcined at 950 °C, additional and dissimilar to the commented HA Raman peaks, other peaks are observed at 409, 974 and 1015 cm^{-1} corresponding to the PO^{3-}_4 v_2, v_1 and v_3 modes of β-tricalcium phosphate (β-Ca3(PO4)2:β-TCP), respectively [21]. The spectrum of the powder calcined at 600 °C shows a low intensity peak at 1114 cm^{-1}, that is not observed in the spectrum of the powder calcined at 950 °C and can be related to the presence of organic material (C-H).

The powder calcined at 600 °C consisted entirely of HA phase with well defined peaks, as can be seen from Fig. 7, where the XRD patterns of the fish bones powders are compared with that of HA. There is no difference in XRD patterns between the two studied species. Nevertheless, as can be seen from Fig. 8, the XRD patterns of the powders calcined at 950 °C reveal minor presence of β-tricalcium phosphate (β-$Ca_3(PO_4)_2$:β-TCP) apart from HA, which still constitutes the main component of the resulting powder. Estimation of β-TCP content in the Xiph calcined at 950 °C according to standard ISO-13779:3 revealed a weight percentage value of 13.0 ± 1.5. All the main diffraction peaks have a slight shift towards higher degrees with respect to synthetic HA indicating the change in the unit cell parameters due to substitutions. Calculations of parameter ratio c/a can be used to estimate the carbonate content in B-type HA by means of a quantitative XRD method established by LeGeros [22]. This empirical method (see Fig. 9) relates the cell parameter ratio c/a with the stoichiometric coefficient value x:

$$x = 6(30.383\ c/a – 22.208)^{3/4}.$$

The carbonate content can be then estimated by the obtained x considering the B-type HA chemical formula:

$$Ca_{10-x/2}(PO_4)_{6-x}(CO_3)_x(OH)_2.$$

Table 1
Elemental composition determined by ICP-OES (% w/w).

Sample	Calcination temperature (°C)	Ca	K	Mg	Na	P	Sr	Ca/P (molar)
Thun	600	41.84	0.03	0.31	0.63	17.34	0.07	1.87 ± 0.02
Xiph	600	41.80	0.05	0.32	0.57	17.37	0.07	1.86 ± 0.02
Thun	950	42.31	0.01	0.22	0.39	17.33	0.06	1.89 ± 0.02
Xiph	950	41.75	0.02	0.40	0.51	17.45	0.09	1.84 ± 0.02

Note: the error of the values is 2%.

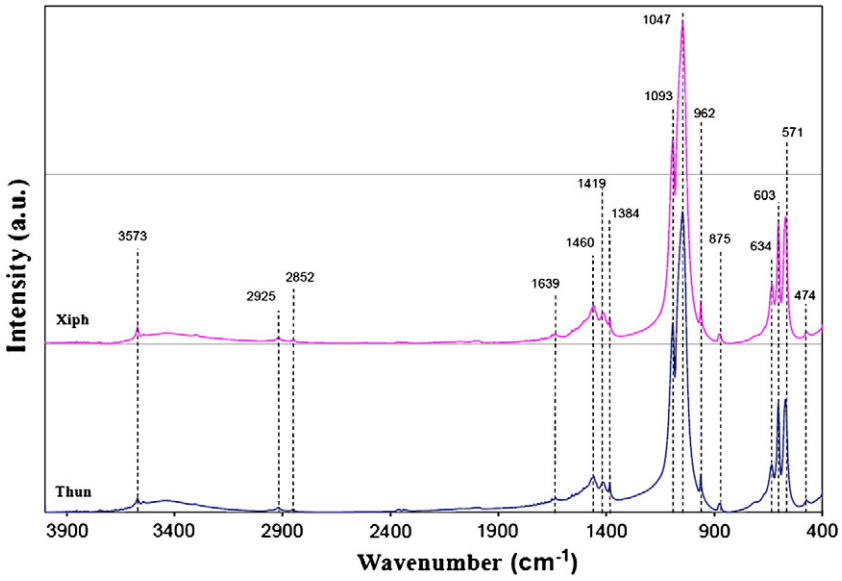

Fig. 3. FTIR spectra of HA obtained from fish bones at 600 °C.

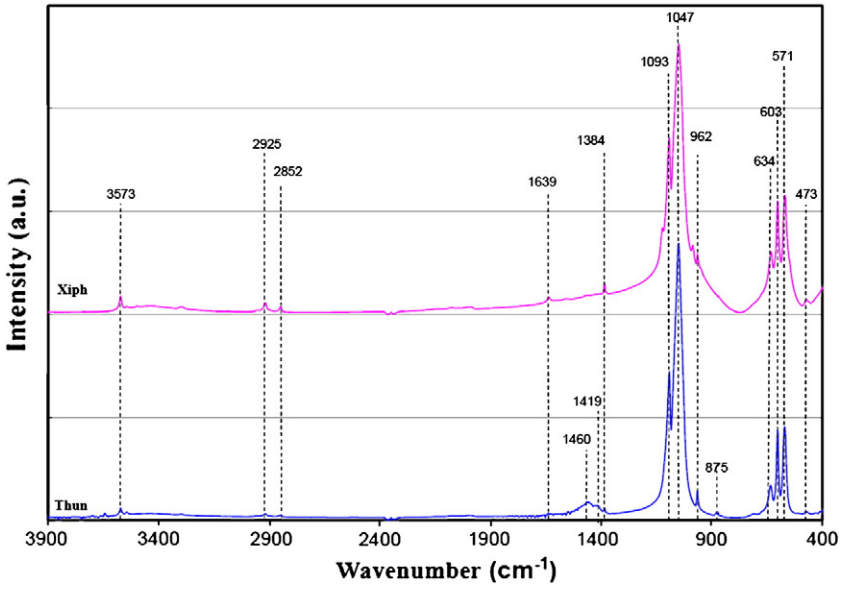

Fig. 4. FTIR spectra of HA obtained from fish bones at 950 °C.

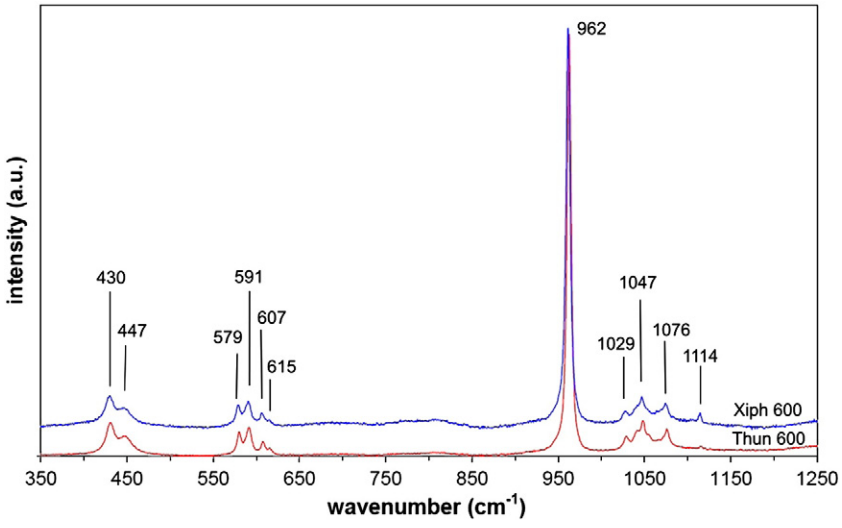

Fig. 5. Raman spectra of HA obtained from fish bones at 600 °C.

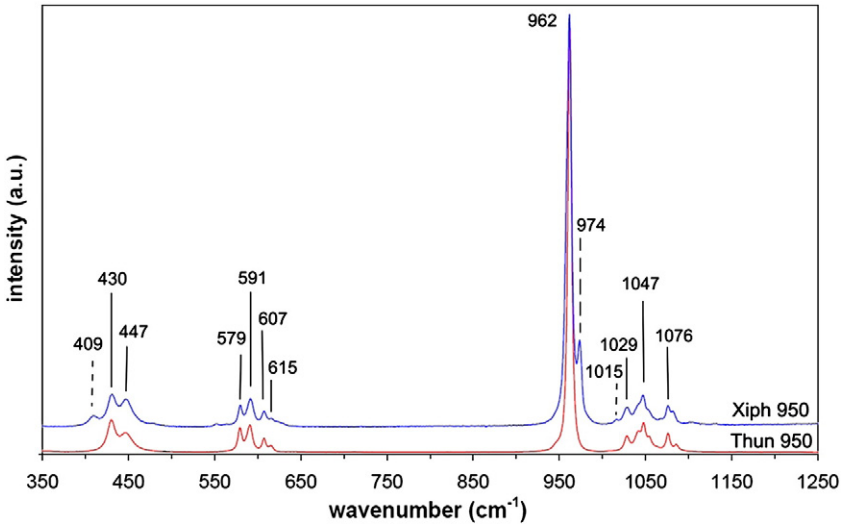

Fig. 6. Raman spectra of HA obtained from fish bones at 950 °C.

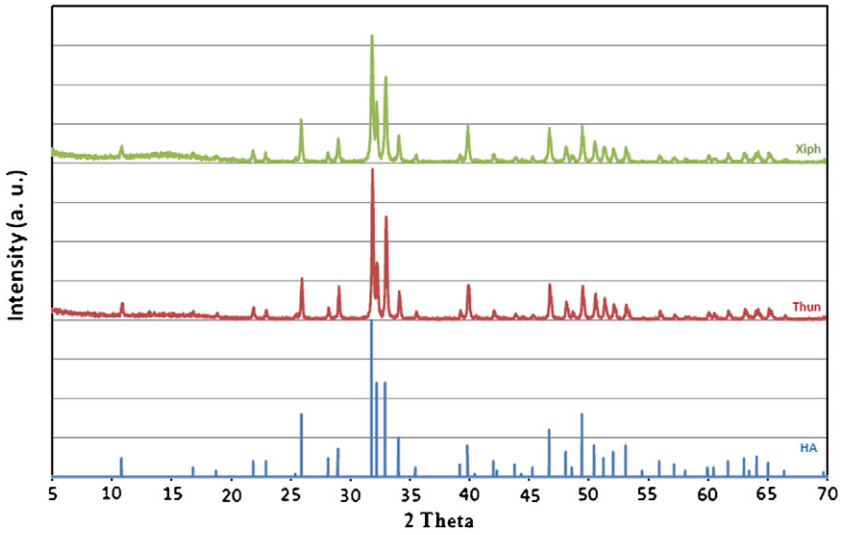

Fig. 7. XRD patterns of fish bones calcined at 600 °C compared with stoichiometric hydroxylapatite (HA: stoichiometric hydroxylapatite from JCPDS-ICDD 1993).

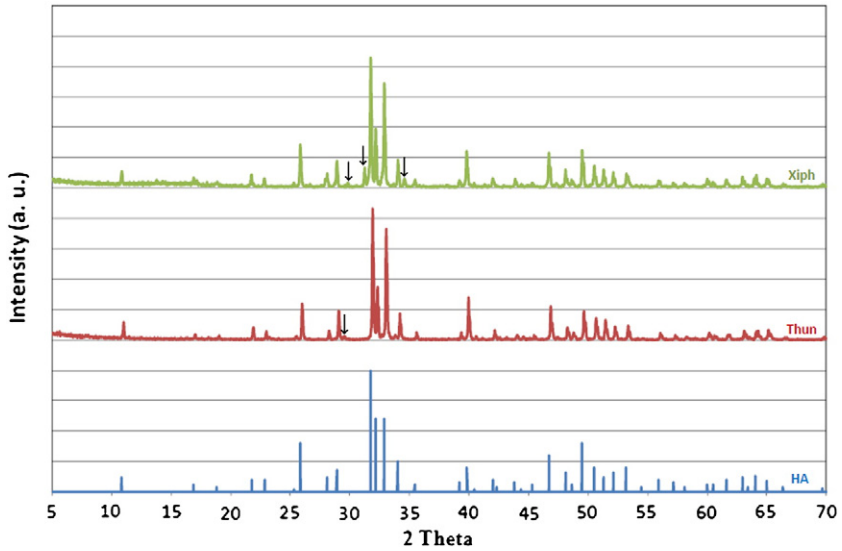

Fig. 8. XRD patterns of fish bones calcined at 950 °C compared with stoichiometric hydroxylapatite (↓: presence of β-TCP, HA: stoichiometric hydroxylapatite from JCPDS-ICDD 1993).

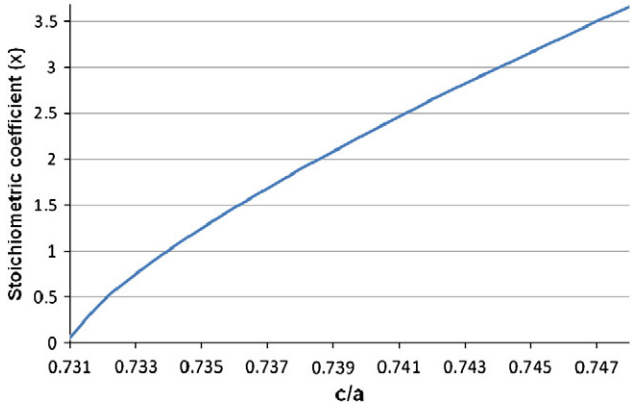

Fig. 9. Relationship between stoichiometric coefficient (x) of the B-type HA chemical formula $Ca_{10-x/2}(PO_4)_{6-x}(CO_3)_x(OH)_2$ and the *c*/*a* ratio.

The variation of cell parameters compared to those of synthetic HA consisted in a decrease in the *a* parameter from 9.418 (ICCD no 9-432) to 9.397 and 9.377 nm in the case of Thun samples calcined at 600 and 950 °C respectively; and an increase in the *c* parameter from 6.884 (ICCD no 9-432) to 6.891 and 6.863 nm for the same samples (see Table 2). With regard to Xiph samples calcined at 600 and 950 °C the *a* parameter changes to 9.408 and 9.425 nm respectively while *c* parameter increased to 6.901 and 6.890 nm.

The *c*/*a* calculated ratio for Thun and Xhip calcined at 600 °C is around 0.7333 and 0.7335 respectively, higher than that of HA (0.7309), and giving the corresponding carbonate content of 5.2% and 5.5%. The *c*/*a* ratio values obtained for the same samples calcined at 950 °C are 0.7318 and 0.7311 respectively resulting in carbonate amounts of 2.5% and 0.6% for Thun and Xiph respectively.

The crystallite size of particles can be approximately calculated from the XRD patterns by means of Scherrer's equation [23]

$$t = \frac{k\lambda}{\beta cos\theta}.$$

where *t* is the average dimension of crystallites in a direction normal to the diffracting plane *h k l*; β is the full width of the peak at half maximum intensity (in radians) located at 2θ; λ is the wavelength of X-ray radiation (1.5418 A) and *k* is the Scherrer constant related to crystallite shape, that falls in the range 0.87–1.0 (it is usually assumed to be 1). It may be assumed that *t*, *cosθ* and *k* values are constant for the same reflection. In this case the mean crystallite size was evaluated using the line broadening of the (2 1 1) reflection, since this peak is well resolved and shows no interferences. The average size of powder crystallites is calculated and the results are tabulated in Table 3.

The crystal size in the obtained powders of the two species at 600 °C is around 50 nm, while it increases to 66 nm at 950 °C. This result is in accordance with the sharpness and the intensity increase of the XRD peaks when the temperature is increased from 600 to 950 °C.

The cytotoxicity results are shown in Fig. 10. In the MTT assay the cells after incubation with the extracts of the test materials produced large amount of coloured formazan indicating that all tested materials were non-cytotoxic. None of the materials had detrimental effect on cellular activity at 100% of extract concentration.

Table 2
Calculated cell parameters and the corresponding amount of carbonates.

Sample	Calcination temperature (°C)	*a* axis (nm)	*c* axis (nm)	*c*/*a*	% CO^{2-}_3
Thun	600	9.397	6.891	0.7333	5.2
Xiph	600	9.408	6.901	0.7335	5.5
Thun	950	9.377	6.863	0.7318	2.5
Xiph	950	9.425	6.890	0.7311	0.6

Table 3
FWHM of the (211) and average crystallite size of the powders obtained from fish bones at 600 and 950 °C.

Sample	Calcination temperature (°C)	FWHM of 211 peak (2θ: 31.8°)	Crystal size (nm)
Thun	600	0.172	54 ± 10
Xiph	600	0.197	47 ± 10
Thun	950	0.138	67 ± 16
Xiph	950	0.141	66 ± 16

4. Discussion

It has been reported by several researchers that HA obtained from animal bones is biologically more active compared to the synthetic one. It seems that this advantage is related to properties inherited from the raw material, such as low crystallinity, nanometric crystal size, and chemical composition including the presence of substituent elements such as Mg^{2+}, K^+, Na^+, etc. [24,25]. The size and morphology of the crystals play an important role in biomechanical function of bone, since the hierarchical assembly and the orientation of the HA crystals in the collagen contribute to the high toughness of the bone. As can be seen from the FSEM and TEM micrographs displayed in Fig. 1, the obtained powders exhibit a rod-like shape which probably are formed by fusion of fundamental blocks as suggested by Eppell et al. [26] showing a preferential crystalline orientation. This rod-like shape instead of the acicular shape typical for stoichiometric apatites can be attributed to the coupled CO^{2-}_3 for PO^{3-}_4 and Na^+ for Ca^{2+} substitutions that cause changes in the size and shape of the apatite crystal: from acicular to rod-like shape crystals [27].

The size and shape of nanoparticles obtained from biogenic hydroxyapatite can preserve important characteristics such as good bioactivity and flexible structure [28,29]. However the heating temperature should be controlled, since recrystallization can lead to growth of crystallite to slightly higher values than those reported for bones to be around 5–20 nm width by 60 nm length [30] and change the original tissue architecture.

The higher molar Ca/P ratio obtained in our material compared to that of the stoichiometric HA, can be attributed to the presence of carbonate ions substituting the phosphate, indicating the presence of B-type carbonate hydroxyapatite. This type of hydroxyapatite is typical of the mineral phase of biological apatites [31] where the carbonates can strongly contribute to the variation of Ca/P ratio. Other authors have also observed higher Ca/P ratio in hydroxyapatite from bovine bones [32]. The incorporation of carbonate ions substituting for phosphates can be crucial, since it has been reported that A-type apatites (i.e. CO^{2-}_3 substituting for OH^-) showed lower affinity for the human trabecular osteoblastic cells, leading to lower cell attachment and collagen production compared with stoichiometric HA [33,34]. Indeed, the presence of B-type carbonate hydroxyapatite in our fish bone materials is confirmed by the FTIR spectra. The peak at 875 cm^{-1} can be assigned to the bending mode and it is present in both, A and B types of carbonate hydroxyapatite [35]. The peaks at 1639, and 1384 cm^{-1} can be assigned to stretching mode of carbonate ions, while the peaks at 1460 and 1419 cm^{-1} are associated to bending mode in B type for carbonate hydroxyapatite due to the substitution of PO^{3-}_4 by the CO^{2-}_3 [36,37]. This is in accordance with the high Ca/P ratio obtained by ICP-OES corroborating the presence of carbonate substituting phosphate ions. The CO^{2-}_3 bands intensity at 1419, 1460 and 1654 decreases or disappears when the calcination temperature increases to 950 °C probably due to the carbonate decomposition to carbon dioxide, which can occur at temperatures ranging from 750 to 1100 °C [38]. This fact would mean that lower calcination temperature

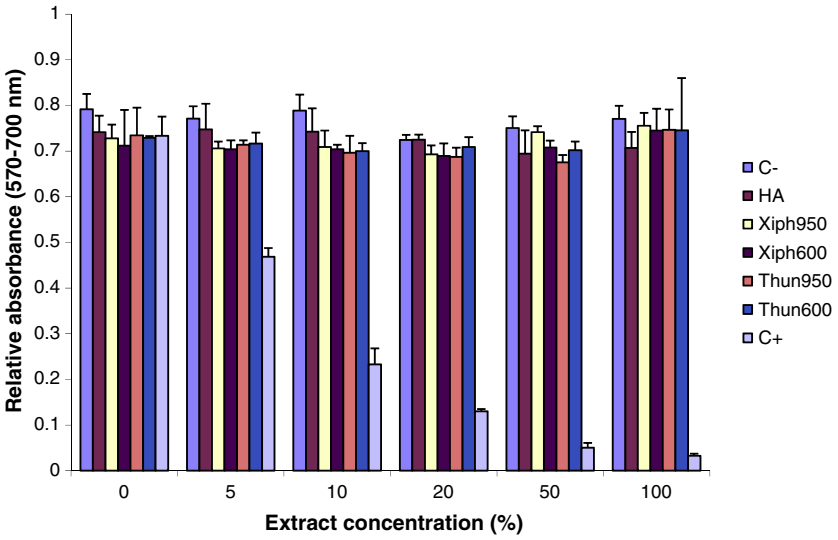

Fig. 10. Relative formation of formazan by MC3T3-E1 cells after incubation with the samples together with commercial HA and control extracts for 24 h. C^+: positive control. C^-: negative control.

should be more appropriate for conserving the carbonate content. The Raman spectra obtained are compatible with the carbonate B-type substitution determined from FT IR and Ca/P ratio measurements. Contribution of carbonate peak at 1073 cm^{-1} overlaps with the phosphate v_3 peak at 1076 cm^{-1} and cannot be separated. Moreover, the lack of carbonate peak at 1100 cm^{-1} allows to rule out A-type carbonate substitution.

The obtained powders are composed of crystalline phases, where the crystallite size measured from the (211) reflection is around 50 nm for the powder calcined at 600 °C, which is in a good agreement with the average crystallite size in mature bone [39]. The nanostructure of bone-substituting materials is closely related to the good bioactivity and osteoconductivity, such behaviour has been observed in synthetic HA composed of nanosized crystals which lead to an increase of osteoblast functions [40]. Moreover, in the presence of HA nanocrystals endothelial cells maintain biochemical markers of healthy endothelium. They do not acquire a proinflammatory or thrombogenic phenotype, but express markers of functioning endothelium that might contribute to angiogenesis [41]. However, the powders obtained at 950 °C show an increase of the crystallite size because of the long time (12 h) kept at high temperature. Similar growth of crystallite has been observed when sheep bones were heated from 500 to 900 °C [42].This tendency suggests again that fish bones heated at 600 °C preserve better the inherited properties from raw material than those calcined at 950 °C.

The elements incorporated to the crystal structure by means of substitutions contribute to changes in lattice parameters due to the difference in ionic radius. The presence of aperiodic spots in the FFT corresponding to HRTEM (see Fig. 2b) might well be due to ions incorporated into the HA structure originating defects. The hexagonal structure of HA contains two different calcium sites. Calcium cations at site I, CaI, are coordinated by nine oxygens belonging to six phosphate anions forming triangles and showing a columnar arrangement. Cations at site II are coordinated by seven oxygen atoms, six belonging to phosphate anions and one to hydroxyl anion. CaI atoms are strictly aligned in columns and any small change in the metal–oxygen interactions affects the entire lattice. However, the CaII atoms belonging to consecutive layers are staggered, allowing random local misplacements without compromising the whole structure. When substitutions take place, cations smaller than Ca (radius = 0.99 Å) are incorporated preferentially in the HA structure at CaI sites. In contrast, larger cations should be incorporated in position CaII [43,44]. In our powders, elements with smaller radius (Mg, 0.66 Å and Na = 0.96 Å) might well be accommodated in site CaI, while those with higher radius (Sr, 1.13 Å and K, 1.33 Å) are better accommodated in CaII sites.

When carbonates are integrated in the HA structure, the smaller CO_3^{2-} volume compared to the substituted PO_4^{3-} radical, leads to a decrease of the *a* parameter and an increase of the *c* parameter of the crystal unit [45]. The contraction of the *a* axis dimensions of the powders compared to HA reveals the presence of the small planar $CO^{2-}{}_3$ replacing the larger tetrahedral PO_4^{3-} group [46]. However, the *a* dimension difference with respect to HA is reduced for the powders calcined at 950 °C, as shown in Table 2, this effect is due to the decomposition of carbonates when the temperature is increased, although some part of carbonate ions move from phosphate to hydroxyl sites, resulting in a small increase in the *a* parameter value [47]. The present results demonstrate that the amount of carbonate, around 5 wt.% in the powder obtained at 600 °C, is similar for both species and it is in the range attributed to bone mineral [48]. Thus, through XRD we corroborated quantitatively the results observed with FTIR with regard to an important loss of carbonate when the calcination temperature is raised from 600 °C to 950 °C. According to the results of the present study, 600 °C seems to be a more appropriate calcination temperature to ensure a carbonate amount in the obtained powders similar to that of the biological HA. This material would respond to the following chemical formula:

$$(Ca, M)_{9.63}(PO_4)_{5.25}(CO_3)_{0.75}(OH)_2$$

where M represents Na, Mg, K and Sr. The presence of these ions is usual in biological apatites. These elements play a significant role on the behaviour of biological apatites, since they contribute to metabolism in human body and cell adhesion. Sodium and magnesium play an important role on bone metabolism and osteoporosis [49,50]. Mg plays a crucial role in cell proliferation and function. Cells are unable to proliferate in the absence of extracellular Mg because of the resultant reduction in DNA, RNA and protein synthesis [51]. While strontium is associated in reducing bone resorption and increasing bone formation leading to the prevention of the risk of fractures [52].

The presence of β-TCP detected in the XRD patterns and in Raman spectra demonstrates that, above certain threshold of heating temperature, biphasic powder from fish bones can be obtained due to partial transformation of HA to β-TCP. Similar results have been obtained by other authors when enamel was heated to 700 °C [53] and animal bones were heated to 800 °C [54]. This biphasic calcium

phoshate, generally comprising a mixture of non-resorbable hydroxyapatite and resorbable β-TCP, has been reported as suitable material for synthetic bone substitute applications because the HA provides a permanent scaffold for new bone formation via osteoconduction while the resorption of the β-TCP oversaturates the local environment with Ca^{2+} and PO^{3-}_4 ions to accelerate the new bone formation [55,56]. The increase of calcination temperature to 950 °C leads to an increase of crytallinity which can be observable in the sharpness and a slight intensity increase of the XRD peaks from the powders obtained at 950 °C. This effect is also confirmed by the increase of crystallite size values to about 67 nm.

Taking into account the strong efficiency of HA to store heavy metals by means of changing cations or adsorbing not changeable ones on the crystal surface [57], it is important to consider the amount of possible toxic elements in the anorganic part of fish bones of both species captured in North Atlantic fishing-grounds. In our samples the concentration of the studied heavy metals (Pb, Cd and Hg) was below the limit established by the American Society for Testing and Materials (ASTM) for anorganic bone for surgical implants [58]. The presence of nontoxic amounts of heavy metals is supported by the results of the MTT assay, showing that the effect of obtained powders is non cytotoxic and similar to that of the commercial hydroxyapatite.

Despite the mandatory tests necessary to be accomplished prior to any use of the reported materials as bone substitutes, these fish bone derived calcium ortophosphates present a promising future. On one hand, sword fish (*X. gladius*) and tuna (*T. thynnus*) are among the biggest fisheries in the world (10,000 Tm of sword fish and 25,000 Tm in the case of tuna are caught each year (average) according to data from the National Oceanic and Atmospheric Administration of USA). Therefore this is a sustainable source of calcium phosphate which is not in danger as coral sources are and which is not linked to the potential transmission to humans of the bovine spongiform encelopathy (BSE) or the new variant of the Creutzfeldt Jakob Disease when using bone substitute of bovine origin (even if it has been already demonstrated that the use of these type of materials does not carry a risk of transmitting BSE to patients [59]).

On the other hand, the use of a biological hydroxyapatite containing Mg as bone substitute, instead of a synthetic one without it, allows maintaining the extracellular amount of Mg at the right level in order to allow a proper cell proliferation which is crucial for bone defect healing [51].

5. Conclusions

Biological hydroxyapatite has been obtained from fish bones available as fishing activities waste. The obtained powders consisted in B type carbonate hydroxyapatite showing higher Ca/P ratio than that of stoichiometric one due to carbonate ions substituting phosphates. The calculated increase of the *c*/*a* ratio to estimate the amount of carbonates in B type carbonate HA resulted in an amount of about 5% of carbonates for powders calcined at 600 °C, similar to carbonate content in human bones. The presence of minor elements such as Na, K, Mg and Sr substituting Ca was also detected. The fish bones calcined at 600 °C resulted entirely in B type carbonate HA, however when the calcination temperature increases to 950 °C, β-TCP appeared in minor amount and the carbonate content decreases according to the FTIR results and *c*/*a* ratio change, indicating a partial decomposition of the material. The MTT assay revealed that all the materials tested were non-cytotoxic.

These fish bone derived calcium ortophosphates present a promising future because the raw material are wastes from a sustainable and cheap source, while the use of a biological substituted apatite containing Mg and Sr as bone substitutes, instead of synthetic apatite without them, would be much beneficial for bone defect healing.

Acknowledgements

The authors gratefully acknowledge the collaboration of the company Fandicosta, S.A. (Moaña, Spain) for providing the fish wastes and the assistance of the technical staff of CACTI (Universidade de Vigo). Authors would also like to thank Prof. Racquel Z. LeGeros (College of Dentistry, New York University) for her fruitful discussions and support at the early stages of this work.

This work was partially supported by the European Union program POCTEP project (0330_IBEROMARE_1_P), the Spanish government (CICYT/FEDER MAT2006-10481) and by Xunta de Galicia (INCITE09E2R303103ES).

References

[1] T. Rustad, Electron. J. Environ. Agric. Food Chem. 2 (2003) 458–463.
[2] W. Suchanek, M. Yoshimura, J. Mater. Res. 13 (1998) 94–117.
[3] L.L. Hench, J. Am. Ceram. Soc. 74 (1991) 1487–1510.
[4] S.M. Best, A.E. Porter, E.S. Thian, J. Huang, J. Eur. Ceram. Soc. 28 (2008) 1319–1327.
[5] H.M. Kim, Y. Kim, S.J. Park, C. Rey, H.M. Lee, M.J. Gimcher, J.S. Ko, Biomaterials 21 (2000) 1129–1134.
[6] T. Leventouri, Biomaterials 27 (2006) 3339–3342.
[7] S.V. Dorozhkin, Acta Biomater. 6 (2010) 715–734.
[8] S.H. Rhee, Biomaterials 23 (2002) 1147–1152.
[9] A. Siddharthan, S.K. Seshadri, T.S. Sampath Kumar, Trends Biomater. Artif. Organs 18 (2005) 110–113.
[10] U. Vijayalakshmi, S. Rajeswari, Trends Biomater. Artif. Organs 19 (2006) 57–62.
[11] A. Ito, S. Nakamura, H. Aoki, M. Akao, K. Teraoka, S. Tsutsumi, K. Onuma, T. Tateishi, J. Cryst. Growth 163 (1996) 311–317.
[12] M.K. Herliansyah, M. Hamdi, A. Ide-Ektessabi, M.W. Wildan, J.A. Toque, Mater. Sci. Eng. C 29 (2009) 1674–1680.
[13] M. Boutinguiza, F. Lusquiños, R. Comesaña, A. Riveiro, F. Quintero, J. Pou, Appl. Surf. Sci. 254 (2007) 1264–1267.
[14] M. Boutinguiza, F. Lusquiños, A. Riveiro, R. Comesaña, J. Pou, Appl. Surf. Sci. 255 (2009) 5382–5385.
[15] J.H.G. Rocha, A.F. Lemos, S. Agathopoulos, P. Valério, S. Kannan, F.N. Oktar, J.M.F. Ferreira, Bone 37 (2005) 850–857.
[16] ISO 13779-3:2008 "Implants for surgery-hydroxyapatite — Part3: chemical analysis and characterization of crystallinity and phase purity"
[17] D.G.A. Nelson, J.D.B. Featherston, Calcif. Tissue Int. 34 (1982) 69–81.
[18] I.U. Rehman, R. Smith, L.L. Hench, W. Bonfield, Bioceramics 7 (1994) 80–84.
[19] Z. Movasaghi, S. Rehman, I.U. Rehman, Appl. Spectrosc. Rev. 42 (2007) 493–541.
[20] G. Penel, G. Leroy, C. Rey, E. Bres, Calcif. Tissue Int. 63 (1998) 475–481.
[21] H. Li, B.S. Ng, K.A. Khor, P. Cheang, T.W. Clyne, Acta Mater. 52 (2004) 445–453.
[22] R.Z. LeGeros, in: H. Myers (Ed.), Calcium Phosphates in Oral Biology and Medicine. Monographs in Oral Sciences, vol. 15, Karger, Basel, 1991, pp. 82–107.
[23] A.L. Patterson, Phys. Rev. 56 (1939) 978–982.
[24] M.P. Ferraz, F.J. Monteiro, C.M. Manuel, J. Appl. Biomater. Biomech. 2 (2004) 74–80.
[25] W. Linhart, F. Peters, W. Lehmann, K. Schwarz, A.F. Schilling, M. Amling, J.M. Rueger, M. Epple, J. Biomed. Mater. Res. 54 (2001) 162–171.
[26] S.J. Eppell, W. Tong, J. Lawrence Katz, L. Kuhn, M.J. Glimcher, J. Orthop. Res. 19 (2001) 1027–1034.
[27] R.Z. LeGeros, J.P. LeGeros, in: L.L. Hench, J. Wilson (Eds.), An introduction to Bioceramics, World Scientific, Singapore, 1993, pp. 139–180.
[28] J. Huang, Y.W. Lin, X.W. Fu, S.M. Best, R.A. Brooks, N. Rushton, W. Bonfield, J. Mater. Sci. Mater. Med. 18 (2007) 2151–2157.
[29] J. Chevalier, L. Gremillard, J. Eur. Ceram. Soc. 29 (2009) 1245–1255.
[30] W. Paul, C.P. Sharma, Am. J. Biochem. Biotechnol. 2 (2006) 41–48.
[31] A. Antonakos, E. Liarokapis, T. Leventouri, Biomaterials 28 (2007) 3043–3054.
[32] S. Joschek, B. Nies, R. Krotz, A. Göpferich, Biomaterials 21 (2000) 1645–1658.
[33] S.A. Redey, S. Razzouk, C. Rey, D. Bernache-Assollant, G. Leroy, M. Nardin, G. Cournot, J. Biomed. Mater. Res. 45 (1999) 140–147.
[34] S.A. Redey, M. Nardin, D. Bernache-Assollant, C. Rey, P. Delannoy, L. Sedel, P.J. Marie, J. Biomed. Mater. Res. 50 (2000) 353–364.
[35] T.S.B. Narasaraju, D.E. Phebe, J. Mater. Sci. 31 (1996) 1–21.
[36] R.Z. LeGeros, G. Bonel, J.P. LeGeros, Calcif. Tissue Res. 26 (1978) 11–118.
[37] I. Mayer, S. Schneider, M. Sydney-Zax, D. Deutsch, Calcif. Tissue Res. 46 (1990) 254–257.
[38] S.M. Barinov, J.V. Rau, S.N. Cesaro, J. Durisin, I.V. Fadeeva, D. Ferro, L. Medvecky, G. Trionfetti, J. Mater. Sci. Mater. Med. 17 (2006) 597–604.
[39] M.J. Olszta, X. Cheng, S.S. Jee, R. Kumar, Y.Y. Kim, M.J. Kaufman, E.P. Douglas, L.B. Coger, Mater. Sci. Eng., R 58 (2007) 77–116.
[40] G. Balasundaram, M. Sato, T.J. Webster, Biomaterials 27 (2006) 2798–2805.
[41] S. Pezzatini, R. Solito, L. Morbidelli, S. Lamponi, E. Boanini, A. Bigi, M. Ziche, J. Biomed. Mater. Res. A 76 (2006) 656–663.
[42] J.C. Hiller, T.J.U. Thompson, M.P. Evison, A.T. Chamberlain, T.J. Wess, Biomaterials 24 (2003) 5091–5097.
[43] Z.Y. Li, W.M. Lam, C. Yang, B. Xu, G.X. Ni, S.A. Abbah, K.M.C. Cheung, K.D.K. Luk, W.W. Lu, Biomaterials 28 (2007) 1452–1460.
[44] E. Boanini, M. Gazzano, A. Bigi, Acta Biomater. 6 (2010) 1882–1894.

[45] T. Leventouri, J. Mater. Res. 16 (2001) 2600–2606.
[46] R.Z. LeGeros, Nature 206 (1965) 403–404.
[47] T.I. Ivanova, O.V. Frank-Kamenetskaya, A.B. Koltsov, V.L. Ugolkov, Solid State Chem. 160 (2001) 340–349.
[48] F.C.M. Driessens, Bioceramics of Calcium Phosphates, CRC Press, Boca Raton, FL, 1983, pp. 1–32.
[49] M. Šarić, M. Piasek, M. Blanuša, K. Kostial, J.Z. Ilich, Nutrition 21 (2005) 609–614.
[50] I.R. Gibson, W. Bonfield, J. Mater. Sci. Mater. Med. 13 (2002) 685–693.
[51] R.K. Rude, H.E. Gruber, J. Nutr. Biochem. 15 (2004) 710–716.
[52] P.J. Marie, Bone 38 (2006) 10–14.
[53] J. Shi, A. Klocke, M. Zhang, U. Bismayer, Eur. J. Mineral. 17 (2005) 769–776.
[54] L.D. Mkukuma, J.M.S. Skakle, I.R. Gibson, C.T. Imrie, R.M. Aspden, D.W.L. Hukins, Calcif. Tissue Int. 75 (2004) 321–328.
[55] M. Vallet-Regí, J.M. González-Calbet, Prog. Solid State Chem. 32 (2004) 1–31.
[56] E. Goyenvalle, E. Aguado, J.M. Nguyen, N. Passuit, L. Le Guenennec, P. Layrolle, G. Daculsi, Biomaterials 27 (2006) 1119–1128.
[57] T. Moriguchi, S. Nakagawa, F. Kaji, Phosphorus Res. Bull. 22 (2008) 54–60.
[58] Annual Book of ASTM Standards, F 1581-99. Standard Specification for Composition of Anorganic Bone for Surgical Implants.USA: ASTM; 1999; 13(01): 893–895.
[59] B. Wenz, B. Oesch, M. Horst, Biomaterials 22 (2001) 1599–1606.